Monolithically MEMS Laser Beam Steering Fabricated on AlGaAs System

Carlos F.R. Mateus

***Abstract* — A torsional structure for monolithical laser beam steering is proposed. The steering part of the device is a torsional actuator and an edge emitting laser is integrated to the torsional beam. The device steers the laser beam in the direction perpendicular to the substrate.**

***Index Terms* — Optoelectronic devices, optical networks, DWDM systems, optical MEMS, laser display, optical switch.**

I. Introduction

Laser beam steering is very attractive for many modern applications such as image sensing, laser displays and optical switches for fiber networks. Different methods have been investigated. Monolithically fabricated scanning have been achieved by various devices by means of liquid crystals [1], current guiding [2], electrooptic [3] and phased arrays [4]. However, the scanning aperture is usually smaller than would be possible using a moving structure. Mechanical scanning have been demonstrated by different types of silicon-based MEMS mirrors [5, 6] and waveguides [7, 8]. Although silicon-based MEMS mirrors can be fabricated in small scale, integration with laser diode is necessary in order to achieve laser beam steering. As a result, silicon-based MEMS devices inhibit higher costs due to the requirement for high accuracy in surface mounting and beam alignment.

Monolithic beam steering is limited in the number of resolvable spots in the far field due to diffraction loss from the laser aperture. As such, it is unlikely that a monolithic laser beam steering device will compete with bulk optics beam steering techniques in this field. However, low cost and increased optical capacity, allowing parallel transmission of multiple channels, are very attractive [9].

In this article I propose a torsional MEMS structure monolithically integrated with an edge emitting laser (EEL), which has etched facets, capable of scanning the laser beam in the vertical direction. The EEL with dry-etched mirrors was proposed and demonstrated a few years ago [10] and the mechanical torsional part has been recently used in AlGaAs to work as a tunable filter [11]. The device has separated contacts for laser bias and mechanical actuation and a common ground. The purpose of the paper is to establish guidelines on how these two structures can be integrated, define the processing steps and simulate the performance.

Carlos F. R. Mateus is with the Department of Electrical Engineering and Computer Science, University of California, Berkeley, CA, 94720, USA (phone (510) 643-2330, e-mail: mateus@photonics.eecs.berkeley.edu).

II. Device Structure

The device schematic is shown in Fig. 1. The epitaxy layers are deposited over a GaAs semi-insulator substrate and the layers sequence is shown in Table 1. The laser layers are on top of the structure and after processing, an air gap is formed between the laser and the substrate. When a voltage is applied between the top (n-doped) and bottom (p-doped) surfaces (mechanical actuation contacts), the entire structure experiences an electrostatic force pulling it towards the substrate. However, by design, the position of the center of mass lies in the counterweight; the laser beam moves upward whereas the counterweight moves down. Fig. 1 (b) illustrates a cross-section of the device along the laser arm direction. With the output located at the end of the beam, the laser output light will scan in the vertical direction. By appropriately choosing the length ratio of the laser arm and the counterweight, a leveraging effect can be achieved, as illustrated by Fig. 1 (b).

The laser is a gain-guided stripe one. An oxide aperture confines the current but there is no lateral heterobarrier to provide a potential well for carriers or photons. However, the current will not be constant along the device width but will have a gradient distribution being maximum at the center of the beam. As the material gain is proportional to the injected current and it is connected to the index of refraction through the Kramers-Kronig relation, the index of refraction will also be larger at the center of the beam. This change in the index of refraction serves as a guide but light is weakly confined and optical losses tend to be high. An alternative to this is to have a ridge waveguide laser but the increase in processing complexity is not recommended for this very first trial.

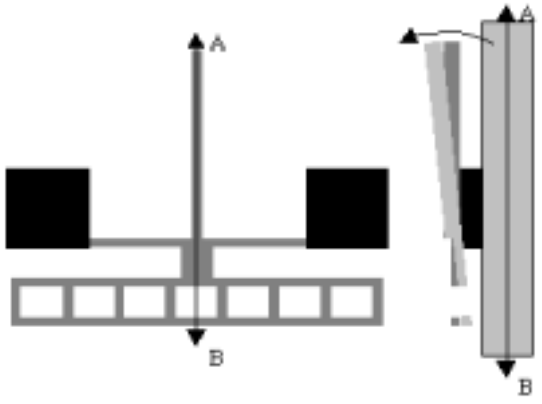

(a) (b)

Fig. 1 - (a) Top view and (b) side view along the laser beam direction of the torsional MEM structure. The sacrificial layer under the gray region in (a) is selectively removed whereas that under the dark region remains.

Table 1 – Layer structure starting from the top.

Material	*Thickness (μm)*	*Doping ($10^{18}/cm^3$)*
GaAs (p- laser contact)	0.2	p – 5
AlAs (current confinement)	1	—
$Al_{0.4}Ga_{0.6}As$ (cladding)	1.8	p – 1
GaAs/InGaAs QW (active)	0.3	—
$Al_{0.4}Ga_{0.6}As$ (cladding)	2	n – 1
GaAs (n- laser/mechanical contact)	1	n – 5
$Al_{0.4}Ga_{0.6}As$ (etch stop)	1	—
GaAs (sacrificial)	7	—
$Al_{0.4}Ga_{0.6}As$ (etch stop)	3	—
GaAs (p- bottom mechanical contact)	1	p – 5
$Al_{0.4}Ga_{0.6}As$ (etch stop)	2	—
GaAs (substrate)	—	—

Two pairs of contacts are necessary: one for mechanical actuation and another for laser bias. The intermediary n-contact layer serves as ground for both laser and mechanical bias and its pad is on the anchor as is the p- laser contact. Eventhough both laser contacts pads are on the anchor, injection of current is allowed only along the laser beam, not in the torsion beam, by means of an oxide-isolation layer, which is going to be fully oxidized along the last. The bottom mechanical contacts are on the substrate.

A. Fabrication

Fabrication involves five photolithography steps, three metal depositions, plasma and wet etch and CO_2 critical point drying. The laser beam is 7µm wide and 175µm long. The torsion beams (connected to the contacts) are 80µm long and 5µm wide. The counterweight is 260µm x 35µm with seven 15µm x 20µm holes to facilitate the release etch and is connected to the torsion beams through a 15µm x 14µm beam.

The wafer would be grown by MOCVD on semi-insulating GaAs substrate. The total thickness would be 19.3μm including (from top) a 5.8μm P-I-N edge-emitting laser, with 3 InGaAs quantum wells, emitting at a wavelength of 970nm, a 1μm $Al_{0.4}Ga_{0.6}As$ etch stop layer, 7μm intrinsic GaAs sacrificial layer, a 3μm $Al_{0.4}Ga_{0.6}As$ stop layer, a 1μm GaAs bottom p-contract for mechanical bias and a 2μm $Al_{0.4}Ga_{0.6}As$ etch stop layer.

First in the processing, a 3µm wide stripe, which is the laser current injection region, is etched along the laser beam by wet etching (using HCl) and the top n-contact metal is deposited. The device is then patterned and etched down to the p-bottom mechanical contact layer using $SiCl_4$ reactive ion etching under low pressure. This dry etch gives smooth and vertical mirrors for the laser facets [10]. Another photolithography defines the laser p-contact and the anchor is then etched down to the n- laser/mechanical contact layer. A final photolithography can be made for both mechanical contacts (one on the anchor and the other on the substrate) and the same metal composition (Ti/Au) can be deposited on both. If applied voltage is of concern, two different depositions (and photolithographies) would be necessary as increased resistance at the n- interface is expected for this contact alloy. High temperature wet oxidation will then take place to block the current in the torsion beam. As oxidation is usually run at high temperatures, it will also anneal the contacts. Selective dry etch using a mixture of $SiCl_4$ and SiF_6 gases releases the device. As the last step, critical point drying with CO_2 is necessary as the device has to be cleaned after the release etch.

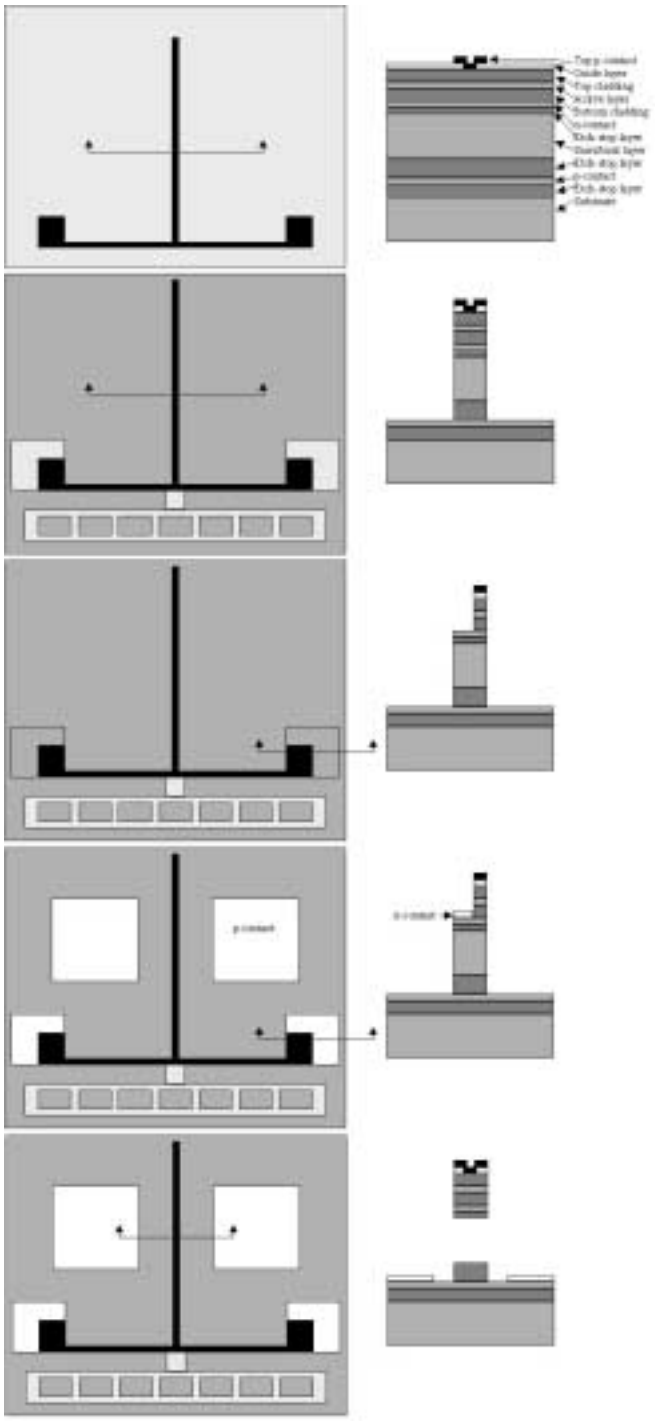

Fig. 2 – Top view and cross-section of the fabrication steps. Starting from top, top laser contatct, device vertical etch, anchor etch for contact, contact deposition and selective release etch.

III. Test Structures

Dimensions were defined in order to have reasonable sizes for processing. If the laser injection current stripe is defined to have 3 μm, the laser beam has to have at least 7μm (extra 2μm on each side of the stripe) for effective gain guiding. The torsion beam is defined to have 5μm for a reasonable aspect ratio of 3:1 during processing. The counterweight is at most 50μm far from the torsion beam in order to have an steering angle of 3.5º (gap is 7μm $\Rightarrow \theta_{max} = \tan^{-1}(gap/d) \approx 8º \Rightarrow \theta_{pull\text{-}in} = 0.44\theta_{max} \approx 3.5º$). This angle is comparable with the usually achievable with other techniques [1 – 4]. The variables that we can play with are the laser beam length, the torsion beam length and the counterweight length.

The laser beam has to have at least 150μm for reasonable optical gain per pass (typical commercial products are between 200 and 500μm). The torsion beam has a trade off between torsion (the longer the better) and bending (the shorter the stiffer) as it is expected to bend a little when voltage is applied. The counterweight can then be designed to have around 75% of the device area, making the torsion easier at low voltages. Table 2 gives the proposed test structures.

Table 2 – Test structures (μm).

#	*Laser beam*	*Torsion beam*	*Counterweight*
1	150	80	260
2	175	80	260
3	200	80	260
4	175	60	260
5	175	100	260
6	175	80	225
7	175	80	295

IV. Expected Results

The performance of the device can be calculated by considering the rectangular beam torsional spring constant:

$$k_{torsional} = \frac{Etw(t^2 + w^2)}{24(1+\nu)l} \tag{1}$$

where E is Young's modulus, t is thickness, w is width, l is length and ν is Poisson's ratio. The torque appplied to the beam due to electrostatic actuation is given by:

$$\tau = \frac{1}{2}\varepsilon_0 V^2 \frac{A^2 d}{g^2} \tag{2}$$

where ε_0 is air pemitivitty, V is applied voltage, g is gap size, A is area and d is the distance from the surface with area A to the beam. In our case the product A^2d should be replaced by the integral:

$$\int_{connector} w_{con} x dx + \int_{counterweight} w_c x dx - \int_{laser\ beam} w_l x dx \tag{3}$$

where w_{con}, w_c and w_l are the widths of the connector, counterweight and laser beam, respectively, as each element of area contribute to the torque proportionally to its width. The steering angle can then be calculated as a function of the applied voltage:

$$\theta_{steering} = \frac{\tau}{k_{torsional}} \tag{4}$$

However, this calculation does not take into account the bending of the beams which will determine the "external steering" or the effective angle that the laser spot is going to describe in the far field. In order to accurately determine the performance of device, two different softwares were used: Sugar and FEMLAB. Sugar is a CAD for MEMS developed in University of California, Berkeley, with very easy interface for fast simulations [12]. FEMLAB is a finite element tool with full graphical interface.

Two of the simulation outputs, one from each software, both for structure # 2 from Table 2, are shown in Fig. 3. They are amplified to show the details. Bending of both torsion and laser beams may be critical if their lengths are large. The counterweight also bends and the maximum torsion is achieved when the extreme of the counterweight moves $\theta_{pull\text{-}in}$ (3.04μm) towards the substrate.

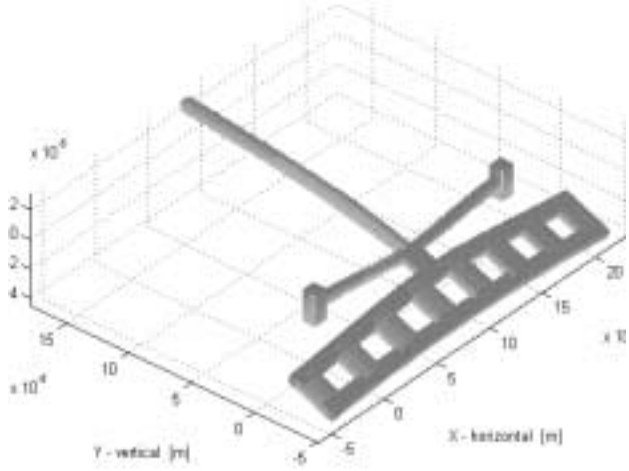

(a)

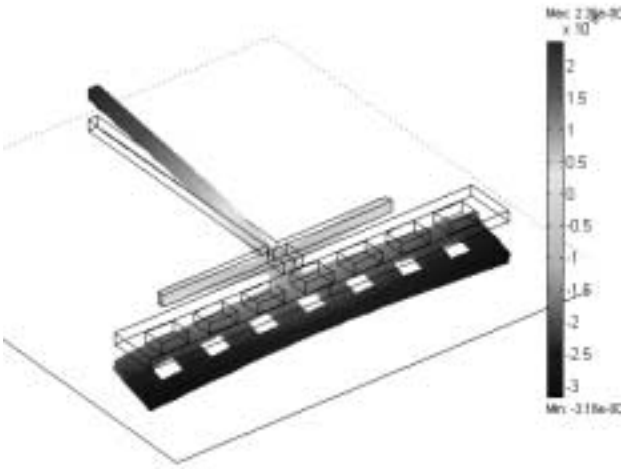

(b)

Fig. 3 – Example of simulated results for (a) sugar and (b) FEMLAB. The images are exaggerated to show details.

The different test structures were simulated and the results are shown in Table 3. To simulate using Sugar, a constant force were distributed over several points along the device, proportionally to the area, and this force were increased until the pull-in point, as defined above, were achieved. The displacement of the tip of the laser beam is reported in Table 3. The procedure was similar for FEMLAB but the force was distributed per area and the solution was calculated using non-linear iteration as function of the gap size. It is interesting to note that FEMLAB used approximately half the force than Sugar to achieve pull-in.

Table 3 – Displacement (μm) of the tip of the laser as the counterweight reaches the maximum deflection for the different test structures of Table 2.

#	*Sugar*		*FEMLAB*	
	Δz (μm)	Force (μN)	Δz (μm)	Force (μN)
1	3.5	880	2.98	440
2	2.7	880	2.45	480
3	0.88	1000	0.66	540
4	2.0	1150	2.10	632
5	2.7	700	2.21	370
6	3.0	1000	2.22	580
7	2.2	750	2.61	450

The steering angle can then be calculated based on the tip displacement:

$$\theta_{steering} = \tan^{-1}\left(\frac{\Delta z}{laser\ beam\ length}\right) \quad (5)$$

The largest angle was achieved for structure #1, where Sugar gave an angle of 1.34º and FEMLAB 1.15º. This is much less than expected but previous experience with this torsional device in GaAs shows that the laser beam bending is not this large at least when the device has a DBR structure [11]. That device was a vertical tunable filter and had a large area at the tip of the beam for light coupling and even with a large electrostatic force being applied at the tip, its displacement was double than the counterweight and no bending was noticed. In mine simulations, the tip displacement was always less than the counterweight, exception for #1 simulated with Sugar, what shows the need of fabricating different test structures to analyze the device.

Looking at the results in Table 3, is possible to understand the trade-offs for this device. Shorter laser beams will give larger steering angles (see #s 1 to 3) because they will suffer less electrostatic attraction and will bend less than the large ones. As the concern here is steering, shorter beams would be desirable. The disadvantage of shorter beams is the low optical gain per pass which may cause the laser efficiency to be dramatically reduced.

Longer torsion beams (compare #s 2, 4 and 5) will need smaller voltages to pull-in than the shorter ones. In other obvious words, the twist is larger as the considered section is far away from the anchor. The problem with longer beams, as pointed before, is that they will also bend. This can be noticed when comparing the displacements of #5 (longest torsion beam) and #2 (intermediary): Sugar gives the same displacement and FEMLAB gives a smaller one.

Longer counterweights (compare #s 2, 6 and 7) have more area and will need less voltage to pull-in. However, the extreme laterals will bend towards the substrate and they will be the limiting part of the device. The longer the counterweight is, the more it may bend before twisting the device reasonably and may achieve the pull-in at smaller steering angles. By the other side, the shorter they are, the more voltage they need and this higher voltage may pull the entire structure towards the substrate and cause the resultant angle to be smaller. The real effect is inconclusive from the simulations as Sugar gave the first case and FEMLAB gave the second. Only an experimental test can solve this dilemma.

V. Conclusion

I have demonstrate the feasibility of the monolithical MEMS laser scanner. Simulations show that the scanning angle is much smaller than designed due to bending of both torsion and laser beams. However, previous work using this structure does not show this problem. Different test structures should then be carefully analyzed. This torsional MEMS design can still be conjugated with a lateral actuator sitting in another plane to work as a 2D scanner.

References

[1] H. Okada, P.J. Bos and H. Onnagawa, "In-plane liquid crystal beam steering devices using a beam separation structure", *Jpn. J. Appl. Phys*., Vol. 37, pp 2576-2580, 1998.

[2] X. Dong, P. LiKamWa, J. Loehr and R. Kaspi, "Current-Induced guiding and beam steering in active semiconductor planar waveguide", *IEEE Phot. Tech. Lett*., Vol. 11, no. 7, July 1999.

[3] C.H. Bulmer, W.K. Burns and T.G. Giallorenzi, "Performance criteria and limitations of electrooptic waveguide array deflectors", *Appl. Opt.*, vol. 18, no. 19, pp. 3282-95, 1979.

[4] F. Vasey, F.K. Reinhart, R. Houdre and J.M. Stauffer, "Spatial optical beam steerring with an AlGaAs integrated phased array", *Appl. Opt.*, vol. 32, no. 18, pp. 3220-32, 1993.

[5] R.A. Conant, J.T Nee, K.Y. Lau, R.S. Muller, "A flat high-frequency scanning micromirror", *Solid-State Sensor and Actuator Workshop, Proceedings*, Hilton Head Island, SC, USA, 4-8 June 2000.

[6] A. Tuantranont, et al., "Bulk-etched surface micromachined and flip-chip integrated micromirror array for infrared applications", *2000 IEEE/LEOS International Conference on Optical MEMS, Proceedings*, pp. 69-70, Kauai, HI, USA.

[7] I. Shubin and P. Likamwa, "A guided-wave optical switch controlled by a micro-electro-mecahnical cantilever", *2000 IEEE Annual Meeting Conference, Proceedings*, Rio Grande, Puerto Rico, 13-16 Nov. 2000.

[8] S.M. Jackson, et al., "Optical beam steering using integrated optical modulators", *J. of Lightwave Tech*., Vol. 15, no. 12, 1997.

[9] Francis, D.A.; Chang-Hasnain, C.J.; Kiang, M.-H.; Lau, K.Y.; Muller, R.S., "Beam steering laser arrays and applications in 2D laser scanning.", *1997 Digest of the IEEE/LEOS Summer Topical Meetings*: VCSELs Technologies, Montreal, Canada, 11-15 Aug. 1997.

[10] G.A. Vawter, L.A. Coldren, J.L. Merz and E.L. Hu, "Nonselective etching of GaAs/AlGaAs double heterostructure laser facets by Cl_2 reactive ion etching in a load-locked system", Appl. Phys. Lett. vol. 51, no. 10, pp. 719-21, 1987.

[11] C.F.R. Mateus, L. Chrostowski, C.H.Chang and C.J. Chang-Hasnain, "Widely tunable torsional optical filter", sub. to *IEEE Phot. Tech. Lett.* in Oct. 2001.

[12] Internet: http://www-bsac.eecs.berkeley.edu/cadtools/sugar/